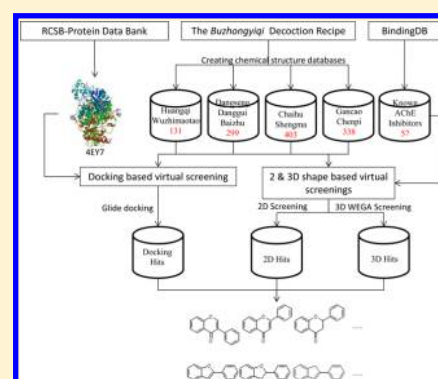


Discovering New Acetylcholinesterase Inhibitors by Mining the *Buzhongyiqi* Decoction Recipe Data

Lu Cui,^{†,||} Yu Wang,^{§,||} Zhihong Liu,[‡] Hongzhuan Chen,[§] Hao Wang,^{*,§} Xinxin Zhou,^{*,†} and Jun Xu^{*,‡}[†]School of Chinese Materia Medica, Guangzhou University of Chinese Medicine, Guangzhou 510006, China[‡]School of Pharmaceutical Sciences, Sun Yat-Sen University, 132 East Circle Road at University City, Guangzhou 510006, China[§]Department of Pharmacology, Institute of Medical Sciences, Shanghai Jiao Tong University, School of Medicine, 280 South Chongqing Road, Shanghai 200025, China

S Supporting Information

ABSTRACT: Myasthenia gravis (MG) is a neuromuscular disease that is conventionally treated with acetylcholinesterase (AChE) inhibitors, which may not fully remove the symptom for many reasons. When AChE inhibitors do not work, Chinese patients turn to Chinese medicine, such as the *Buzhongyiqi* decoction (BD), to treat MG. By elucidating the relations between the herbs of the *Buzhongyiqi* decoction recipe and AChE inhibitors with structure-based and ligand-based drug design methods and chemoinformatics approaches, we have found the key active components of BD. Using these key active components as templates, we have discovered five new AChE inhibitors through virtual screening of a commercial compound library. The new AChE inhibitors have been confirmed with Ellman assays. This study demonstrates that lead identification can be inspired by elucidating Chinese medicine. Since BD is a mixture, further studies against other drug targets are needed.



1. INTRODUCTION

Myasthenia gravis (MG) is characterized by muscle weakness and abnormal fatigability that is usually exacerbated with repeated physical activity and relieved with rest.¹ It is believed that MG is caused by circulating antibodies that block acetylcholine receptors (AChRs) at postsynaptic neuromuscular junctions.^{2–4} In 1934, Mary Walker realized that MG symptoms were relieved when patients were treated with physostigmine, a cholinesterase inhibitor.⁵ Since then, cholinesterase inhibitor therapy became the standard mainstay for symptomatic treatment of MG.⁶ Anti-acetylcholinesterase (anti-AChE) is a symptomatic therapy for MG;^{7,8} anti-AChE slows down the hydrolysis of acetylcholine. Consequently, with anti-AChE treatment, functional AChRs were more stimulated by the retained ACh, so as to improve, in the short term, the conditions of MG patients.⁴ Even now, AChE inhibitors are the recommended first-line and first-step therapy for MG,⁹ as pyridostigmine has been used as a safe treatment for MG for over 60 years.^{10,11}

In Chinese medicine, the *Buzhongyiqi* decoction (BD) has been used to treat MG by Tietao Deng.¹² On the basis of the tradition, the BD recipe consists of four groups of herbs:

- (1) *Jun* (emperor herbs that treat the main cause of MG): Huangqi (*Radix Astragali Mongolici*) and Wuzhimaotao (*Radix Fici Simplicissimae*)
- (2) *Chen* (minister herbs that enhance the actions of *Jun* or treat symptoms): Dangsheng (*Radix Codonopsis*), Danggui (*Radix Angelicae Sinensis*), and Baizhu (*Rhizoma Atractylodis Macrocephalae*)

- (3) *Zuo* (adjuvants that reduce the potential toxicity of the *Jun* or *Chen* herbs and treat symptoms): Chaihu (*Radix Bupleuri*) and Shengma (*Rhizoma Cimicifugae Foetidae*)
- (4) *Shi* (couriers that deliver the herbs to the organs): Gancao (*Radix Glycyrrhizae*) and Chenpi (*Pericarpium Citri Reticulatae*).

Therefore, the *Buzhongyiqi* decoction contains many active components that regulate many drug targets.^{13,14} Consequently, understanding the mechanisms of action of BD and ensuring the quality of Chinese medicine are very difficult.^{15,16} In this work, we used technologies developed by our group, such as virtual screening (VS)¹⁷ and molecular similarity algorithms,^{18–22} to develop a protocol for seeking the BD's active components and their targets. Since there are potentially many active components and targets, to simplify our research we hypothesized that AChE is the primary target for the *Buzhongyiqi* decoction. Our primary questions were the following: (1) Among the *Jun*, *Chen*, *Zuo*, and *Shi* herbs, which are the main herbs acting against the AChE target? (2) With regard to the main herbs acting against AChE, what are the chemical scaffolds for AChE inhibitors? By answering these questions, we have discovered new AChE inhibitors by (1) using the chemical scaffolds derived from the active components of the *Buzhongyiqi* decoction and (2) performing virtual and physical screening of our in-house compound library.

Received: July 18, 2015

Published: October 28, 2015

2. MATERIALS AND METHODS

2.1. Chemical Compositions of *Jun*, *Chen*, *Zuo*, and *Shi* Herbs

A total of 1198 chemical compounds were collected from the Traditional Chinese Medicine Systems Pharmacology Database (TCMSP)²³ and the literature. *Radix Astragali Mongolici* has 87 compounds; *Radix Fici Simplicissimae* has 47 compounds; *Radix Codonopsis* has 134 compounds; *Radix Angelicae Sinensis* has 125 compounds; *Rhizoma Atractylodis Macrocephalae* has 55 compounds; *Radix Bupleuri* has 288 compounds; *Rhizoma Cimicifugae Foetidae* has 119 compounds; *Radix Glycyrrhizae* has 280 compounds; and *Pericarpium Citri Reticulatae* has 63 compounds. The structures of these molecules were downloaded from the TCMSP²³ or prepared using ISIS Draw 2.5. The databases of *Jun*, *Chen*, *Zuo*, and *Shi* herbs contain 131, 299, 403, and 338 chemical structures, respectively.

2.2. AChE Inhibitor Data. A total of 8805 AChE inhibitors were derived from BindingDB.²⁴ After removing the compounds that (1) did not have IC₅₀ data, (2) had duplicated structures, or (3) had IC₅₀ values that were greater than 10 μ M, we arrived at 57 AChE inhibitors (see the [Supporting Information](#)). These AChE inhibitors were used as probes to seek the active compositions of the *Buzhongyiqi* decoction recipe (i.e., the databases for the *Jun*, *Chen*, *Zuo*, and *Shi* herbs).

2.3. Drug-likeness Filtering. Lipinski's rule of five was applied to remove the chemical structures in the chemical structure databases that putatively possess undesired properties for drug-like compounds.^{25–28} The ADMET parameters for Lipinski's rule were calculated using the MOE program (Chemical Computing Group (CCG), Montreal, Canada). The rule predicts that poor absorption or permeation is more likely if a compound has (1) more than five hydrogen-bond donors, (2) more than 10 hydrogen-bond acceptors, (3) a molecular weight greater than 500 Da, and (4) a calculated log *P* (ClogP) greater than 5. For this work, compounds that violated more than two criteria were excluded. The filtered compounds were mainly polysaccharides, which violated at least rules (1) and (3) and sometimes more. The filtering process resulted in 98 compounds for the *Jun* database, 270 compounds for the *Chen* database, 306 compounds for the *Zuo* database, and 331 compounds for the *Shi* database. These compounds were considered as active composition candidates and potential AChE inhibitors.

2.4. Methods for Discovering Active Compositions from the *Buzhongyiqi* Decoction Recipe. Since AChE was assumed to be a major target, the potential active compositions were AChE-inhibitor-like compounds. We employed topological similarity (2D similarity), three-dimensional similarity (3D similarity), and molecular docking methods to identify AChE-inhibitor-like compounds from the *Buzhongyiqi* decoction.

2.4.1. 2D Similarity Method. The 2D structural similarity of a pair of compounds was calculated on the basis of the chemical-environment-encoded dendritic topological fragment (CEEDTF) fingerprints, which were derived from their chemical-structure connection tables (CTs).¹⁸ With this method, we compared the chemical structures in the *Jun*, *Chen*, *Zuo*, and *Shi* databases against the chemical structures in the AChE inhibitor database. Each compound structure *X_i* in the *Buzhongyiqi* decoction was compared against 57 AChE inhibitors in the AChE inhibitor database, which resulted in 57 similarity values; the maximal similarity value was assigned to *X_i*.

2.4.2. 3D Similarity Method. The 3D similarity program used in this work was the weighted Gaussian algorithm (WEGA), in which the molecular shape density is represented as a linear

combination of weighted atomic Gaussian functions. The weight of each atom is a function of the sum of the overlaps between that atom and all of the others.^{19,20} WEGA does not generate molecular conformations. To calculate the conformations of the compounds in the databases, the Caesar module of Discovery Studio, version 3.5 (Accelrys, Inc., San Diego, CA, USA) was employed to sample conformations (the maximal number of conformations was 100) for each AChE inhibitor or candidate compound in the *Buzhongyiqi* decoction recipe. These conformations were energy-minimized with the MOE program. WEGA allows for the computation of shape-based, pharmacophore-based, or combo (both shape- and pharmacophore-based) similarity. For this work, we used the combo 3D similarity calculation. Besides computing the 3D similarities, WEGA generates 3D molecular conformation overlays.

2.4.3. Molecular Docking Method. The potential active compositions proposed with similarity methods were validated by a molecular docking method. The protein target was the *Homo sapiens* AChE (hAChE) crystal structure, which was derived from the RCSB Protein Data Bank (PDB)²⁹ (access code 4EY7). The resolution was 2.35 Å. The docking program was Glide (Schrödinger, LLC, New York, NY, USA).³⁰ The target data were preprocessed (i.e., protonated and optimized with water removed, such that there were fewer than three hydrogen bonds to nonwaters, and then minimized with the OPLS2005 force field, etc.) with the Protein Preparation Wizard in the Maestro program suite (Schrödinger). The native ligand in the crystal structure was used to define the binding site. The dockings were performed using the Glide extra precision (XP) mode, and the ligand was treated as flexible. The native ligand, donepezil, was redocked back to the binding site, and the root-mean-square deviations (RMSDs) of the redocked and native ligand poses were both 0.42 Å, thus indicating that Glide was a capable docking program for this ligand–receptor complex system.

During docking experiments, 10 ligand poses were kept for each hit that was generated from the 2D and 3D similarity searches. The final pose was determined by the best XP-G score in the Glide program.

2.4.4. Selection of Hits for Molecular Docking. The 2D and 3D similarity search hits were selected by using 2D and 3D similarity (Tanimoto coefficient) thresholds of 0.7 and 0.6, respectively. This resulted in 209 hits that were potential hAChE inhibitors, which were then docked to the binding pocket of 4EY7.

2.4.5. Selection of Compounds for the Ellman Assay. The candidate compounds for the Ellman assay were initially determined by a Glide XP-docking score threshold of -9.0 . This resulted in 129 compounds (see the [Supporting Information](#)), which were further refined through scaffold analysis.³¹ The compounds were mainly classified into flavon-like and phenylbenzofuran-like families. Since flavon-like scaffolds are not novel, we conducted a Markush search using a structural query modified from the phenylbenzofuran-like scaffold against the SPECS database, which resulted in 24 phenylbenzofuran-like compounds for the Ellman assay.

2.4.6. Ellman Assay. The Ellman assay³² was used to measure the inhibitory activities of the 24 proposed compounds against hAChE. The 24 virtual hit compounds were diluted in a phosphate buffer (0.08 M Na₂HPO₄ and 0.02 M NaH₂PO₄, pH 8.0) with 0.057 unit/mL hAChE (human recombinant acetylcholinesterase, C1682, Sigma Chemical Co., St. Louis, MO, USA). Each hit compound was incubated with hAChE at

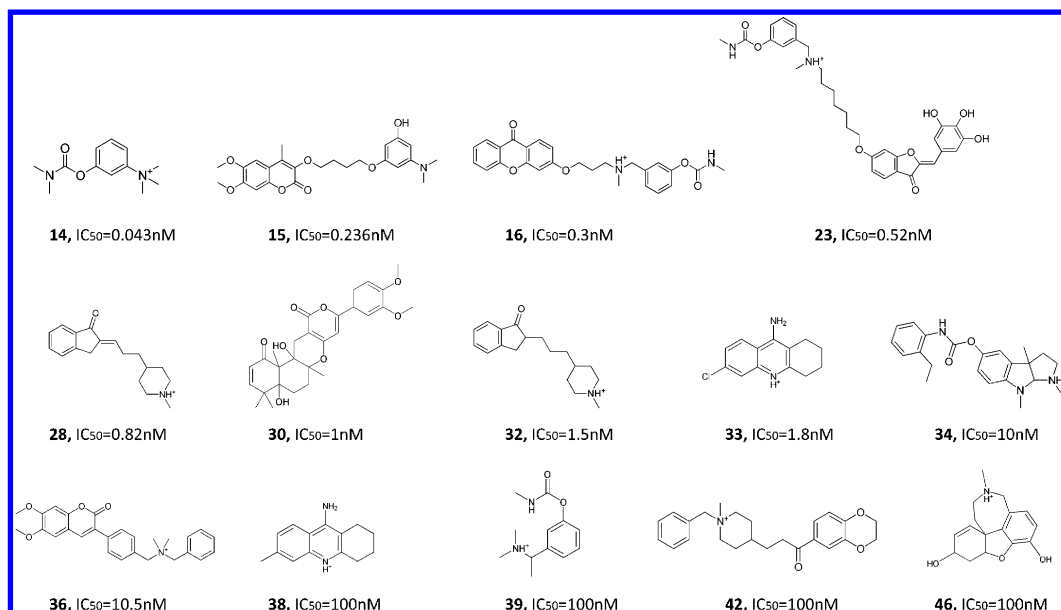


Figure 1. Top 14 AChE inhibitors that were found to be similar to the compounds existing in the *Buzhongyiqi* decoction.

37 °C for 15 min, after which 5,5'-dithiobis(2-nitrobenzoic acid) (DTNB) (D8130, Sigma) was added to a final concentration of 50 μ M. After mixing with acetylthiocholine chloride (ATC) (A5751, Sigma) at 50 μ M, the complex was scanned immediately at 412 nm using a Thermo Scientific Varioskan Flash multimode reader. The inhibitory rate was measured by comparing the absorbance of samples containing compounds with the absorbance in the absence of a test compound. The concentration needed to inhibit 50% of enzymatic activity (IC_{50}) was calculated. Donepezil (D101734, Aladdin Industrial Corporation, Shanghai, China) was used as a positive control. The test and control compounds were both dissolved in dimethyl sulfoxide.

2.4.7. Molecular Dynamics Simulations. The complexes of the ligands with hAChE (derived from PDB code 4EY7) acquired from the docking experiments were analyzed by molecular dynamics (MD) simulations. The complexes were treated with the ff99SB force field³³ and the general AMBER force field³⁴ for proteins and substrates, respectively. Hydrogen atoms were added with LEaP³⁵ from AMBER12. The ligands' partial atomic charges were obtained from the restrained electrostatic potential (RESP) charges based on HF/6-31G* calculations made with the Gaussian 09 package³⁶ and the antechamber suite.³⁷ The systems were solvated in a TIP3P water box with a minimum distance of 8 Å between any protein atom and the edge of the box. The systems were neutralized by adding Na⁺ or Cl⁻ counterions. The side-chain protonation states were assigned using default AMBER protonation states. The MD simulations were run in the AMBER12 package.³⁵ First, 4000 minimization cycles (2000 cycles of steepest descent and 2000 cycles of conjugate gradient) were conducted to relax the solvent, while protein and ligand atoms were constrained by a potential of 3000 kcal mol⁻¹ Å⁻². Second, additional minimization stages were conducted with the protein backbone and the heavy atoms of the substrate constrained (500 kcal mol⁻¹ Å⁻²). Each complex was submitted for 4000 energy minimization cycles without constraints (2000 cycles of steepest descent and 2000 cycles of conjugate gradient). Each complex system was gradually heated from 0 to 300 K over a period of 50 ps, followed by another 100 ps of NPT MD simulation at 300 K. Afterward, 20 ns of NVT MD

simulation with a target temperature of 300 K was performed for each complex to produce a trajectory. The SHAKE algorithm³⁸ was used to constrain the bonds involving hydrogen atoms, and a time step of 2.0 fs was applied for all of the simulations. After 20 ns of MD simulation, the binding free energy (ΔG) was calculated using the molecular mechanics/generalized Born surface area (MM-GBSA) method.³⁹ For each complex, 100 snapshots were extracted from the last 2 ns of the trajectory at intervals of 20 ps.

3. RESULTS AND DISCUSSION

3.1. 2D Similarity Search Results. With a similarity threshold of approximately 70%, 29 hit compounds were found in *Jun* herbs, 35 in *Chen* herbs, 27 in *Zuo* herbs, and 70 in *Shi* herbs. Combining all of the 2D hits, we obtained 137 hit compounds without duplicates. There are 22 known AChE inhibitors (with IC_{50} values ranging from 0.23 nM to 10 μ M) that were found to be similar to the 137 compounds existing in the *Buzhongyiqi* decoction. The top 14 AChE inhibitors (with IC_{50} values ranging from 0.23 to 100 nM) are depicted in Figure 1. The numbers of active components in the *Buzhongyiqi* decoction that are similar to the 22 AChE inhibitors are shown in Figure 2.

Among the 137 active compounds in the *Buzhongyiqi* decoction, 58% (79) are similar to the high-potency AChE inhibitors and 42% (58) are similar to the medium-potency AChE inhibitors. 15 (a coumarin alkaloid) is the most potent AChE inhibitor (IC_{50} = 0.236 nM). Actually, most of the strong AChE inhibitors are alkaloids. The majority of the compounds in the *Jun* and *Shi* herbs of the *Buzhongyiqi* decoction are coumarins and flavonoids. Our similarity search indicates that the functions of *Jun* and *Shi* are due to the compounds that are similar to the coumarin alkaloid-like AChE inhibitors (e.g., compounds 15 and 36 in Figure 1).

3.2. 3D Similarity Search Results. With a similarity threshold of approximately 60%, 24 hit compounds were found in *Jun* herbs, 33 in *Chen* herbs, 27 in *Zuo* herbs, and 41 in *Shi* herbs. Combining all of the 3D hits, we got 108 hit compounds without duplicates. There are 18 known AChE inhibitors (with IC_{50} values ranging from 0.04 nM to 10 μ M) that were found

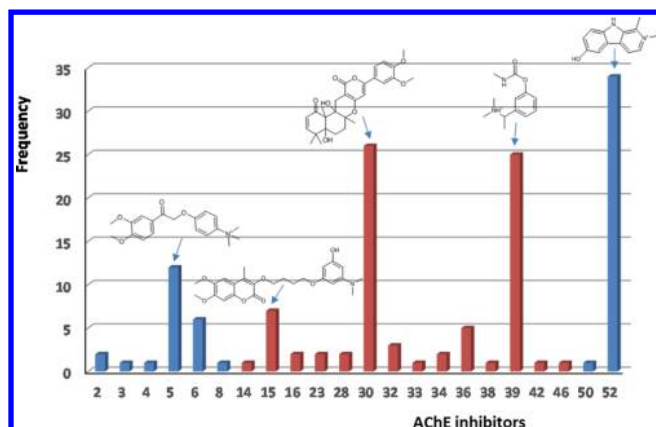


Figure 2. Numbers of active components in the *Buzhongyiqi* decoction that are similar to the 22 AChE inhibitors. The red bars stand for very active AChE inhibitors (i.e., those with IC_{50} values ranging from 0.23 to 100 nM).

to be similar to the 108 compounds existing in the *Buzhongyiqi* decoction. The top 10 AChE inhibitors (with IC_{50} values ranging from 0.04 to 100 nM) are depicted in Figure 3. The numbers of active components in the *Buzhongyiqi* decoction that are similar to the 18 AChE inhibitors are shown in Figure 4. Among the 108 active compounds in the *Buzhongyiqi* decoction, 59% (64) are similar to the high-potency AChE inhibitors and 41% (44) are similar to the medium-potency AChE inhibitors.

3.3. Consensus of 2D and 3D Similarity Search Hits.

The 2D and 3D searches mapped the compounds of the *Buzhongyiqi* decoction onto 22 and 18 known AChE inhibitors, respectively. The 22 known AChE inhibitors included 10 of the 2D-mapped AChE inhibitors. This indicates that the 2D similarity search covers more diverse hits than the 3D search can. Combining the 2D and 3D hits resulted in 209 unique hits, which are the compounds predicted as potential AChE inhibitors in the *Buzhongyiqi* decoction.

3.4. Similarity Hits Finalized through Glide Docking Experiments. The 137 topological similarity search hits and 108 3D similarity search hits were merged. This resulted in 209 unique similarity search hits from the *Buzhongyiqi* decoction that are similar to AChE inhibitors. These hits were docked to an AChE crystal structure. Before conducting docking experiments, we selected the most appropriate docking program and cocrystal hAChE structure through in silico evaluation experiments. We tested the MOE (CCG), Cdocker (Discovery Studio, Accelrys), and Glide (Schrödinger) docking programs

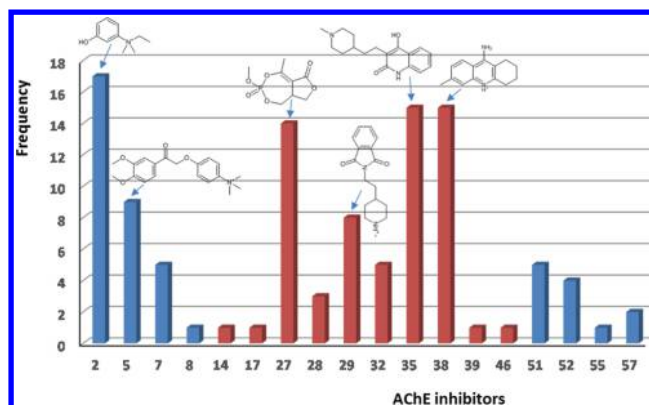


Figure 4. Numbers of active components in the *Buzhongyiqi* decoction that are similar to the 18 AChE inhibitors. The red bars stand for very active AChE inhibitors (i.e., those with IC_{50} values ranging from 0.04 to 100 nM).

with six hAChE cocrystal structures that were retrieved from the PDB. The six native ligands were taken from the binding pockets and docked back to the binding pockets. The RMSDs of the binding poses between the natives and the redocked models are compared in Table 1. The results indicate that the Glide

Table 1. Selection of the Cocrystal Structure and Docking Program

PDB code	resolution	ligand	RMSD (Å)		
			MOE	Cdocker	Glide
4MOE	2.00 Å	dihydrotanshinone I	0.6	0.42	0.24
4MOF	2.30 Å	teritrem B	0.9	0.92	0.56
4BDT	3.10 Å	huprine W	0.61	0.38	0.36
4EYS	2.30 Å	(-)-huperzine A	0.49	3.47	0.20
4EY6	2.40 Å	(-)-galantamine	0.68	0.49	0.20
4EY7	2.35 Å	donepezil	0.91	0.44	0.42

program produced the best docking results for the AChE system and had the lowest RMSDs (ranging from 0.20 to 0.56 Å).

The ligand structures of the cocrystals in Table 1 are depicted in Figure 5A. Donepezil⁴⁰ was the most similar to the chemical structures of the major active compounds found in the *Buzhongyiqi* decoction (Figure 1). Therefore, 4EY7 was selected for the docking experiments because of its flexibility and similarity to the similarity hits.

These compounds can be viewed as the mimicking/bioisostere scaffold of the flavone-like scaffold (Figure 5B).

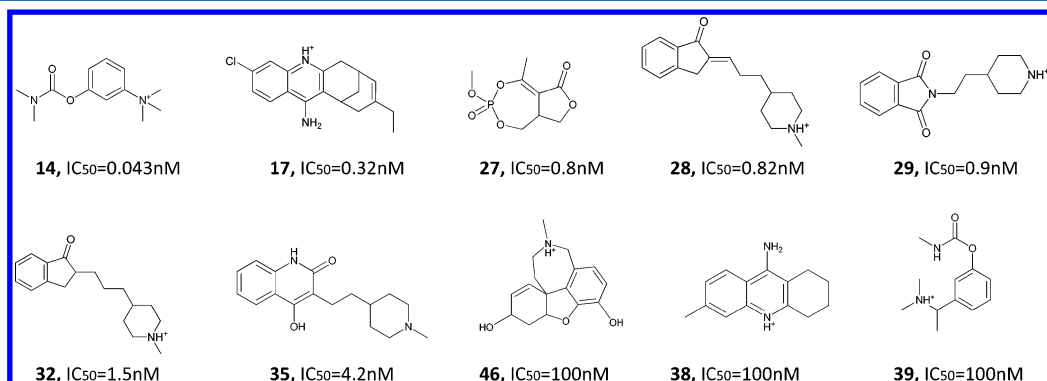


Figure 3. Top 10 AChE inhibitors that were found to be similar to the compounds existing in the *Buzhongyiqi* decoction.

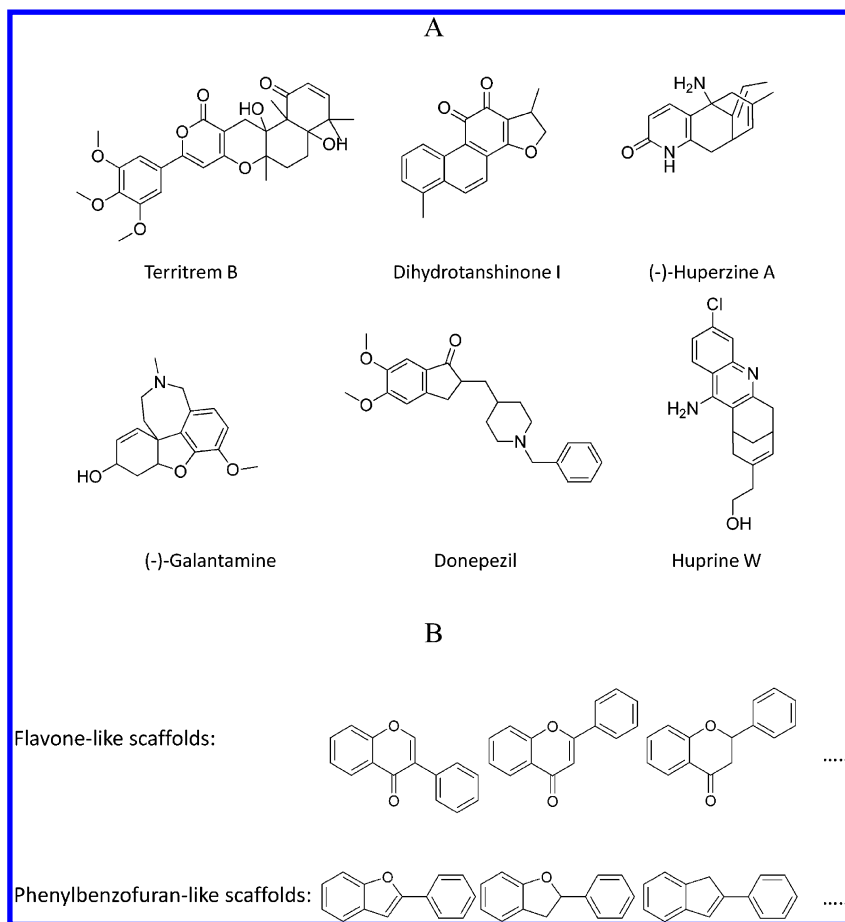


Figure 5. (A) Ligand structures for the six cocrystal structures in Table 1. (B) Main scaffolds existing in the *Buzhongyiqi* decoction compounds that were similar to those of AChE inhibitors.

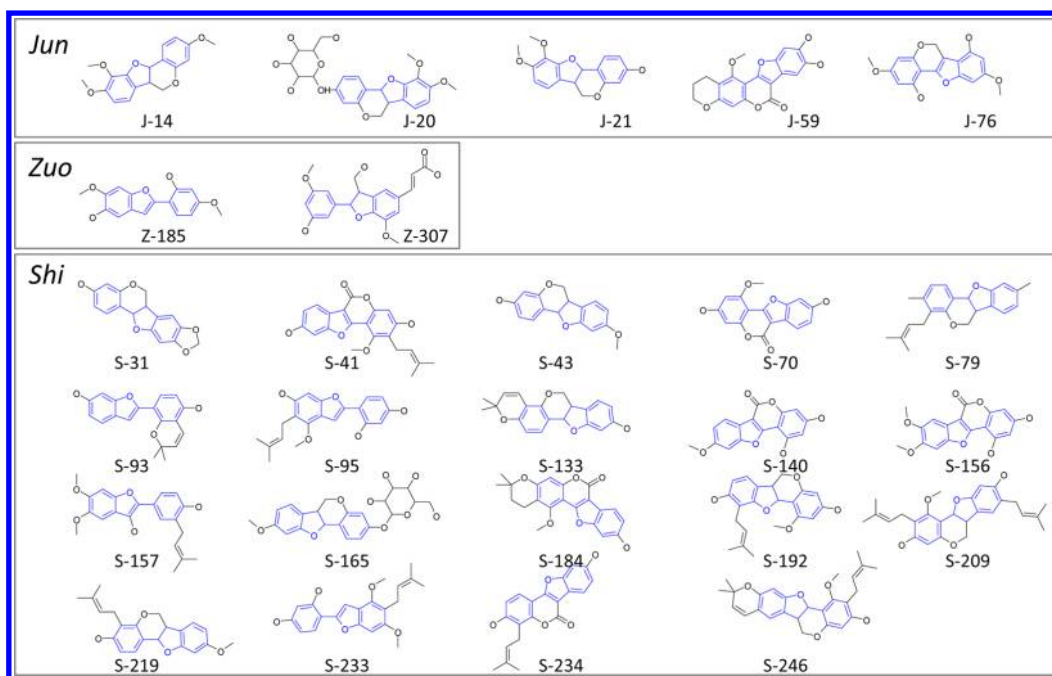


Figure 6. Phenylbenzofuran-like compounds, which are mainly distributed in *Jun* and *Shi* herbs. The scaffold is marked in blue.

Flavone-like compounds have already been reported as AChE inhibitors. For example, Jung and Park⁴¹ reported that quercetin was more than twice as active in inhibiting AChE than

dehydroevodiamine was; Ahmad and colleagues⁴² reported that hispidone significantly inhibits AChE; and Williams and colleagues⁴³ reported nine flavonoid AChE inhibitors from

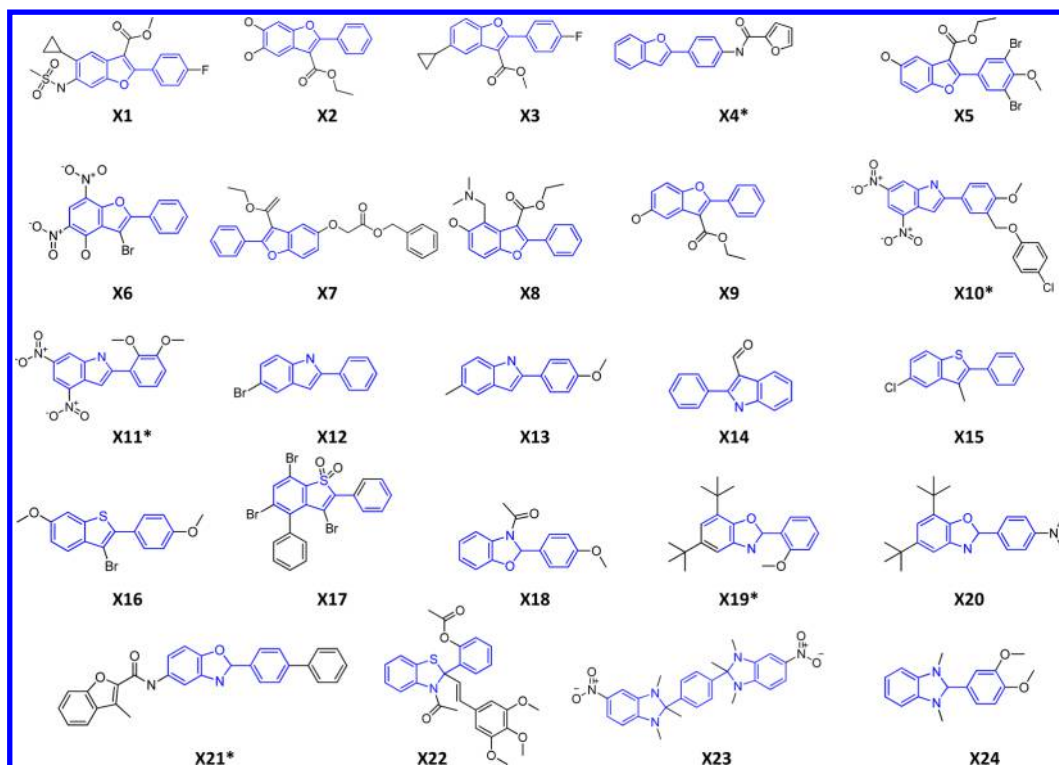


Figure 7. The 24 phenylbenzofuran-like compounds tested with Ellman assays. Active compounds are labeled with asterisks (*).

natural products. The structures of 12 flavonoid and coumarin AChE inhibitors are collected in the [Supporting Information](#).

However, the present study is novel in predicting that phenylbenzofuran-like compounds also can act as AChE inhibitors. The phenylbenzofuran-like compounds in this study are mainly from the *Jun* and *Shi* herbs of the *Buzhongyiqi* decoction (Figure 6). The scaffolds and substituents of active compounds in *Jun* and *Shi* herbs are significantly different. The phenylbenzofuran scaffold is rare in *Zuo* herbs and was not observed in *Chen* herbs. This indicates that *Jun* and *Shi* herbs mainly target AChE; however, compounds in *Chen* and *Zuo* herbs may have different functions within the *Buzhongyiqi* decoction and therefore require further investigation.

3.5. Ellman hAChE Inhibition Assay Results. On the basis of the criteria discussed in section 2.4.5, 24 phenylbenzofuran-like compounds (Figure 7) were determined as final compounds for the Ellman assay. These compounds were acquired from SPECS and tested through Ellman assays for hAChE inhibitory activities. The results are depicted in Figure 8.

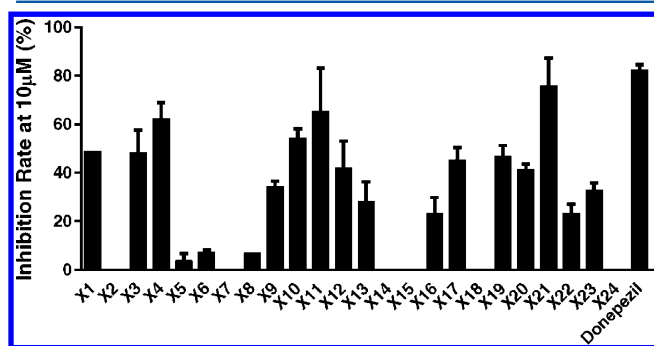


Figure 8. Inhibition of hAChE by the 24 phenylbenzofuran-like compounds at 10 μM.

At 10 μM, five phenylbenzofuran-like compounds exhibited more than 50% inhibition against hAChE. The IC_{50} values of the active compounds were experimentally measured, as shown in Figure 9. Donepezil, which exhibited an IC_{50} value of 30 nM,

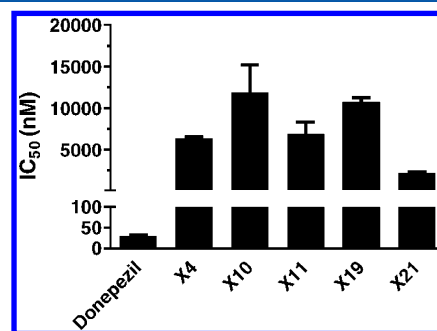


Figure 9. hAChE inhibitory activities of five candidates and the positive control, donepezil.

was used as a positive control.⁴⁴ The most active phenylbenzofuran-like compound is X21 (2.3 ± 0.15 μM). The IC_{50} curves are depicted in the [Supporting Information](#).

3.6. Binding Modes of the Active Compounds. The binding modes and binding free energies of the active compounds were investigated through MD simulations. The RMSDs of the protein backbones indicate that the complexes stabilized after about 20 ns of MD simulation. As shown in Table 2, the predicted binding free energies are consistent with the bioactivity data. A lower ΔG value corresponds to a better IC_{50} value. The ΔG of donepezil (the positive control compound) is -44.52 kcal/mol. Our most active compound, X21 (2.3 ± 0.15 μM), shows the lowest ΔG value of -41.80 kcal/mol, which is comparable with that of donepezil. Compounds X10 and X19, which were predicted to have ΔG

Table 2. Predicted ΔG and Observed IC_{50} Values for hAChE Inhibitors

compound	ΔG_{ele}	ΔG_{vdW}	ΔG_{gas}	AG_{sol}	$\Delta G_{bind,GB}$ (kcal/mol)	IC_{50} (μM)
X4	-17.21 ± 4.77	-37.77 ± 1.51	-54.99 ± 5.44	27.07 ± 3.64	-27.92 ± 2.56	6.5 ± 0.23
X10	97.39 ± 7.76	-46.56 ± 2.00	50.84 ± 8.29	-77.65 ± 7.02	-26.81 ± 3.02	11.4 ± 2.72
X11	-13.21 ± 3.60	-41.84 ± 2.20	-55.05 ± 3.73	24.23 ± 2.89	-30.81 ± 2.76	7.1 ± 1.34
X19	-0.48 ± 2.02	-22.85 ± 3.93	-23.34 ± 4.58	5.98 ± 1.77	-17.35 ± 3.78	10.9 ± 0.48
X21	-24.17 ± 4.26	-52.50 ± 2.87	-76.66 ± 5.27	34.86 ± 2.96	-41.80 ± 3.29	2.3 ± 0.15
donepezil	-149.34 ± 7.63	-47.16 ± 3.02	-196.49 ± 7.15	151.97 ± 7.17	-44.52 ± 2.81	0.031 ± 0.003

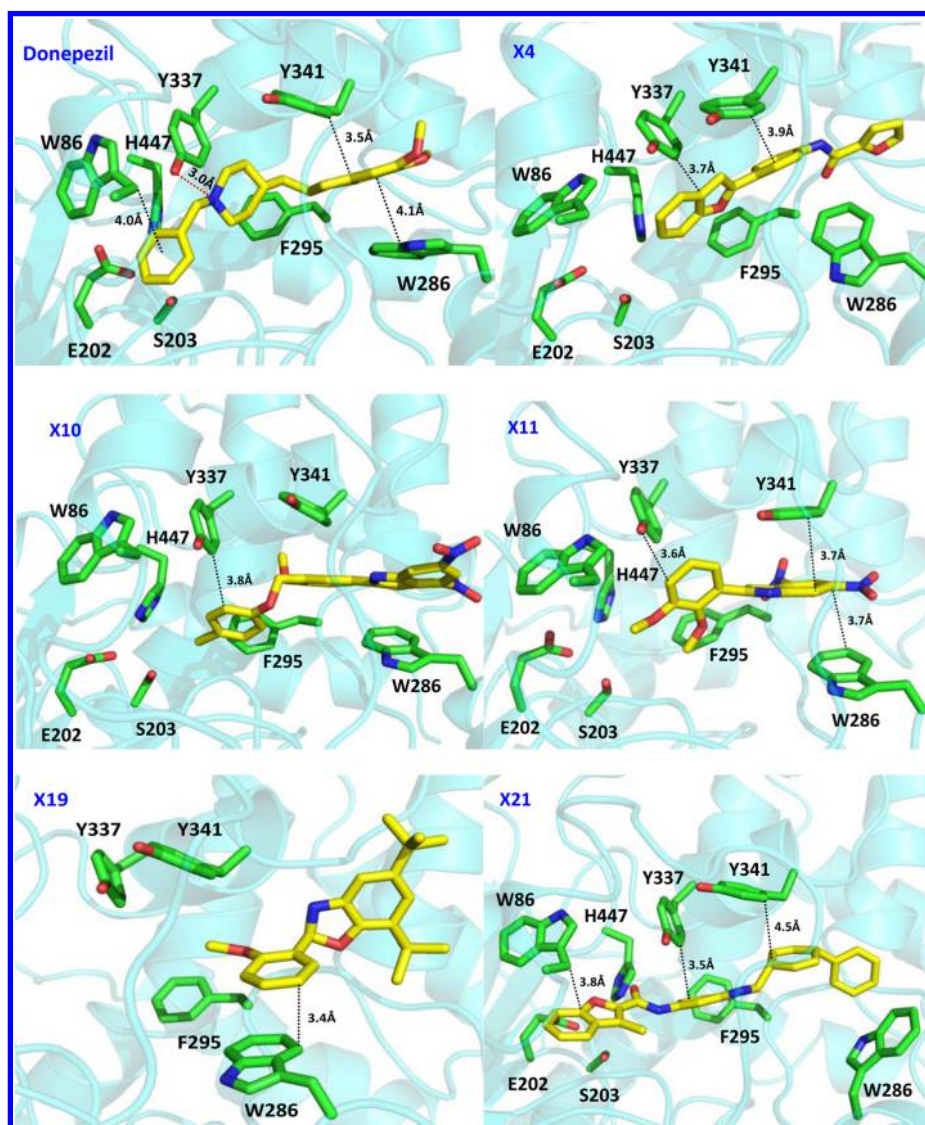


Figure 10. Binding modes for donepezil and the active compounds X4, X10, X11, X19, and X21.

values of -26.81 and -17.35 kcal/mol, had weaker inhibitory activities (their IC_{50} values were -26.81 and -17.35 μM , respectively) as well. The binding modes of donepezil and the five active compounds are illustrated in Figure 10. The native ligand donepezil interacts with Y337 through hydrogen bonding and forms van der Waals interactions with W86, W286, and Y341. These results are consistent with the X-ray cocrystal structure and indicate the important roles of those residues. Other compounds in Table 2 cannot form hydrogen-bonding interactions with Y337. This is probably the main cause of their weaker binding compared with donepezil. The binding abilities of those compounds mainly come from hydrophobic or van der Waals interactions. The benzofuran ring of

X4 forms binding interactions with residue Y337; also, X4's benzene ring interacts with residue Y341. The chlorobenzene of X10 interacts with Y337. X11 interacts with W286, Y337, and Y341. The methoxybenzene of X19 interacts with W286. The three hydrophobic centers of X21 interact with W86, Y337, and Y341, respectively.

4. CONCLUSION

The original goal of this project was to identify the active components of the *Buzhongyiqi* decoction as a treatment for myasthenia gravis disease. We assumed that AChE is the major target. By collecting and mining the AChE inhibitor structural

data and the compound structural data of the *Jun*, *Chen*, *Zuo*, and *Shi* herbs within the *Buzhongyiqi* decoction prescription, we have demonstrated that the active components of the *Buzhongyiqi* decoction mainly exist within the *Jun* and *Shi* herbs. These active components are flavonoid derivatives that act as AChE inhibitors. The molecules of the *Chen* and *Zuo* herbs within the *Buzhongyiqi* decoction may have different functions for treating MG and need further investigation.

By analyzing the structures of active components against AChE, we were able to discover a new class of AChE inhibitors through a scaffold-hopping method and the Ellman assay. The MD simulations gave predicted binding free energy values that are consistent with the bioactivity data for the new AChE inhibitors. This indicates that the binding modes are capable of virtual screening of AChE inhibitors. This study demonstrates that structure-based drug discovery can be inspired by identifying active components from Chinese herbal medicines.

■ ASSOCIATED CONTENT

■ Supporting Information

The Supporting Information is available free of charge on the ACS Publications website at DOI: 10.1021/acs.jcim.5b00449.

Structures and IC₅₀ values of the 57 AChE inhibitors (PDF)

Structures and Glide XP-scores for the 129 Ellman assay candidates obtained using Glide (PDF)

Structures of 12 flavonoid- and coumarin-based AChE inhibitors (PDF)

IC₅₀ plots for X4, X10, X11, X19, X21, and donepezil (PDF)

■ AUTHOR INFORMATION

Corresponding Authors

*E-mail: junxu@biochemomes.com (J.X.).

*E-mail: xinxin_zhou@163.com (X.Z.).

*E-mail: angela_wanghao@hotmail.com (H.W.).

Author Contributions

[†]L.C. and Y.W. contributed equally.

Notes

The authors declare no competing financial interest.

■ ACKNOWLEDGMENTS

This work was supported by the National Natural Science Foundation of China (81173470 and 81473138), the National High Technology Research and Development Program of China (863 Program) (2012AA020307), the National Supercomputer Center in Guangzhou (2012Y2-00048/2013Y2-00045 and 201200000037), the Introduction of Innovative R&D Team Program of Guangdong Province (2009010058), and the Guangdong Provincial Key Laboratory of Construction Foundation (2011A060901014).

■ REFERENCES

- (1) Berrih-Aknin, S.; Frenkian-Cuvelier, M.; Eymard, B. Diagnostic and clinical classification of autoimmune myasthenia gravis. *J. Autoimmun.* **2014**, *48–49*, 143–148.
- (2) Conti-Fine, B. M.; Milani, M.; Kaminski, H. J. Myasthenia gravis: past, present, and future. *J. Clin. Invest.* **2006**, *116*, 2843–2854.
- (3) Berrih-Aknin, S.; Le Panse, R. Myasthenia gravis: a comprehensive review of immune dysregulation and etiological mechanisms. *J. Autoimmun.* **2014**, *52*, 90–100.

(4) Keeseey, J. C. Clinical evaluation and management of myasthenia gravis. *Muscle Nerve* **2004**, *29*, 484–505.

(5) Pearce, J. M. S. Mary Broadfoot Walker (1888–1974): A historic discovery in myasthenia gravis. *Eur. Neurol.* **2005**, *53*, 51–53.

(6) Hughes, T. The early history of myasthenia gravis. *Neuromuscular Disord.* **2005**, *15*, 878–886.

(7) Kumar, V.; Kaminski, H. J. Treatment of Myasthenia Gravis. *Curr. Neurol. Neurosci. Rep.* **2011**, *11*, 89–96.

(8) Schumm, F.; Henze, T. Symptomatic Treatment of Myasthenia Gravis and Other Neuromuscular Transmission Disorders. *Aktuel. Neurol.* **2011**, *38*, 178–189.

(9) Jayam Trough, A.; Dabi, A.; Solieman, N.; Kurukumbi, M.; Kalyanam, J. Myasthenia gravis: a review. *Autoimmune Dis.* **2012**, *2012*, 874680.

(10) Maggi, L.; Mantegazza, R. Treatment of Myasthenia Gravis Focus on Pyridostigmine. *Clin. Drug Invest.* **2011**, *31*, 691–701.

(11) Gilhus, N. E.; Owe, J. F.; Hoff, J. M.; Romi, F.; Skeie, G. O.; Aarli, J. A. Myasthenia gravis: a review of available treatment approaches. *Autoimmune Dis.* **2011**, *2011*, 847393.

(12) Jiang, C.; Liu, P.; Liang, Y.; Qiu, S.; Bao, W.; Zhang, J. Clinical treatment of myasthenia gravis with deficiency of spleen and kidney based on combination of disease with syndrome theory. *J. Tradit. Chin. Med.* **2013**, *33*, 444–448.

(13) Li, X.; Xu, X.; Wang, J.; Yu, H.; Wang, X.; Yang, H.; Xu, H.; Tang, S.; Li, Y.; Yang, L.; Huang, L.; Wang, Y.; Yang, S. A system-level investigation into the mechanisms of Chinese Traditional Medicine: Compound Danshen Formula for cardiovascular disease treatment. *PLoS One* **2012**, *7*, e43918.

(14) Kola, I.; Landis, J. Can the pharmaceutical industry reduce attrition rates? *Nat. Rev. Drug Discovery* **2004**, *3*, 711–715.

(15) Zhao, J.; Jiang, P.; Zhang, W. Molecular networks for the study of TCM pharmacology. *Briefings Bioinf.* **2010**, *11*, 417–430.

(16) Normile, D. Asian medicine. The new face of traditional Chinese medicine. *Science* **2003**, *299*, 188–190.

(17) Ge, H.; Wang, Y.; Li, C.; Chen, N.; Xie, Y.; Xu, M.; He, Y.; Gu, X.; Wu, R.; Gu, Q.; Zeng, L.; Xu, J. Molecular Dynamics-Based Virtual Screening: Accelerating the Drug Discovery Process by High-Performance Computing. *J. Chem. Inf. Model.* **2013**, *53*, 2757–2764.

(18) Yan, X.; Gu, Q.; Lu, F.; Li, J.; Xu, J. GSA: a GPU-accelerated structure similarity algorithm and its application in progressive virtual screening. *Mol. Diversity* **2012**, *16*, 759–769.

(19) Yan, X.; Li, J.; Liu, Z.; Zheng, M.; Ge, H.; Xu, J. Enhancing molecular shape comparison by weighted Gaussian functions. *J. Chem. Inf. Model.* **2013**, *53*, 1967–1978.

(20) Yan, X.; Li, J.; Gu, Q.; Xu, J. gWEGA: GPU-accelerated WEGA for molecular superposition and shape comparison. *J. Comput. Chem.* **2014**, *35*, 1122–1130.

(21) Yan, X.; Ding, P.; Liu, Z.; Wang, L.; Liao, C.; Gu, Q.; Xu, J. Big data in drug design. *Kexue Tongbao (Chin. Ed.)* **2015**, *60*, 558–565.

(22) Zheng, M.; Liu, Z.; Yan, X.; Ding, Q.; Gu, Q.; Xu, J. LBVS: an online platform for ligand-based virtual screening using publicly accessible databases. *Mol. Diversity* **2014**, *18*, 829–840.

(23) Ru, J.; Li, P.; Wang, J.; Zhou, W.; Li, B.; Huang, C.; Li, P.; Guo, Z.; Tao, W.; Yang, Y.; Xu, X.; Li, Y.; Wang, Y.; Yang, L. TCMSP: A database of systems pharmacology for drug discovery from herbal medicines. *J. Cheminf.* **2014**, *6*, 13.

(24) Binding DB—The Binding Database. <http://www.bindingdb.org/> (accessed July 16, 2014).

(25) Klebe, G. Virtual ligand screening: strategies, perspectives and limitations. *Drug Discovery Today* **2006**, *11*, 580–594.

(26) Lipinski, C. A.; Lombardo, F.; Dominy, B. W.; Feeney, P. J. Experimental and computational approaches to estimate solubility and permeability in drug discovery and development settings. *Adv. Drug Delivery Rev.* **2001**, *46*, 3–26.

(27) Quinn, R. J.; Carroll, A. R.; Pham, N. B.; Baron, P.; Palframan, M. E.; Suraweera, L.; Pierens, G. K.; Muresan, S. Developing a drug-like natural product library. *J. Nat. Prod.* **2008**, *71*, 464–468.

(28) Ntie-Kang, F.; Nwodo, J. N.; Ibezim, A.; Simoben, C. V.; Karaman, B.; Ngwa, V. F.; Sippl, W.; Adikwu, M. U.; Mbaze, L. M.

Molecular modeling of potential anticancer agents from african medicinal plants. *J. Chem. Inf. Model.* **2014**, *54*, 2433–2450.

(29) RCSB Protein Data Bank. <http://www.rcsb.org> (accessed May 27, 2014).

(30) Cheung, J.; Rudolph, M. J.; Burshteyn, F.; Cassidy, M. S.; Gary, E. N.; Love, J.; Franklin, M. C.; Height, J. J. Structures of human acetylcholinesterase in complex with pharmacologically important ligands. *J. Med. Chem.* **2012**, *55*, 10282–10286.

(31) Xu, J. A New Approach to Finding Natural Chemical Structure Classes. *J. Med. Chem.* **2002**, *45*, 5311–5320.

(32) Ellman, G. L.; Courtney, K. D.; Andres, V., Jr.; Feather-Stone, R. M. A new and rapid colorimetric determination of acetylcholinesterase activity. *Biochem. Pharmacol.* **1961**, *7*, 88–95.

(33) Hornak, V.; Abel, R.; Okur, A.; Strockbine, B.; Roitberg, A.; Simmerling, C. Comparison of multiple Amber force fields and development of improved protein backbone parameters. *Proteins: Struct., Funct., Genet.* **2006**, *65*, 712–725.

(34) Wang, J. M.; Wolf, R. M.; Caldwell, J. W.; Kollman, P. A.; Case, D. A. Development and testing of a general amber force field. *J. Comput. Chem.* **2004**, *25*, 1157–1174.

(35) Case, D. A.; Cheatham, T. E.; Darden, T.; Gohlke, H.; Luo, R.; Merz, K. M.; Onufriev, A.; Simmerling, C.; Wang, B.; Woods, R. J. The Amber biomolecular simulation programs. *J. Comput. Chem.* **2005**, *26*, 1668–1688.

(36) Frisch, M. J.; Trucks, G. W.; Schlegel, H. B.; Scuseria, G. E.; Robb, M. A.; Cheeseman, J. R.; Scalmani, G.; Barone, V.; Mennucci, B.; Petersson, G. A.; et al. *Gaussian 09W*; Gaussian, Inc.: Wallingford, CT, 2009.

(37) Wang, J. M.; Wang, W.; Kollman, P. A.; Case, D. A. Automatic atom type and bond type perception in molecular mechanical calculations. *J. Mol. Graphics Modell.* **2006**, *25*, 247–260.

(38) Ryckaert, J.-P.; Ciccotti, G.; Berendsen, H. J. C. Numerical integration of the Cartesian equations of motion of a system with constraints: molecular dynamics of *n*-alkanes. *J. Comput. Phys.* **1977**, *23*, 327–341.

(39) Miller, B. R.; McGee, T. D.; Swails, J. M.; Homeyer, N.; Gohlke, H.; Roitberg, A. E. MMPBSA.py: An Efficient Program for End-State Free Energy Calculations. *J. Chem. Theory Comput.* **2012**, *8*, 3314–3321.

(40) Giacobini, E. Cholinesterase inhibitors: new roles and therapeutic alternatives. *Pharmacol. Res.* **2004**, *50*, 433–440.

(41) Jung, M.; Park, M. Acetylcholinesterase inhibition by flavonoids from *Agrimonia pilosa*. *Molecules* **2007**, *12*, 2130–2139.

(42) Ahmad, I.; Anis, I.; Malik, A.; Nawaz, S. A.; Choudhary, M. I. Cholinesterase inhibitory constituents from *Onosma hispidum*. *Chem. Pharm. Bull.* **2003**, *51*, 412–414.

(43) Williams, P.; Sorribas, A.; Howes, M. J. R. Natural products as a source of Alzheimer's drug leads. *Nat. Prod. Rep.* **2011**, *28*, 48–77.

(44) Luo, Z.; Sheng, J.; Sun, Y.; Lu, C.; Yan, J.; Liu, A.; Luo, H. B.; Huang, L.; Li, X. Synthesis and evaluation of multi-target-directed ligands against Alzheimer's disease based on the fusion of donepezil and ebselen. *J. Med. Chem.* **2013**, *56*, 9089–9099.